Published in final edited form as:
Metallomics. 2012 August 25; 4(8): 761–770. doi:10.1039/c2mt20086d.

Changing Iron Content of the Mouse Brain during Development

Gregory P. Holmes-Hampton[a], **Mrinmoy Chakrabarti**[a], **Allison L. Cockrell**[b], **Sean P. McCormick**[a], **Louise C. Abbott**[c], **Lora S. Lindahl**[a], and **Paul A. Lindahl**[a,b,*]

[a]Texas A&M University, Department of Chemistry, College Station, TX 77843 USA

[b]Texas A&M University, Department of Biochemistry & Biophysics, College Station, TX 77843 USA

[c]Texas A&M University, Department of Veterinary Integrative Biosciences, College of Veterinary Medicine and Biomedical Sciences, College Station, Texas, USA

Abstract

Iron is crucial to many processes in the brain yet the percentages of the major iron-containing species contained therein, and how these percentages change during development, have not been reliably determined. To do this, C57BL/6 mice were enriched in ^{57}Fe and their brains were examined by Mössbauer, EPR, and electronic absorption spectroscopy; Fe concentrations were evaluated using ICP-MS. Excluding the contribution of residual blood hemoglobin, the three major categories of brain Fe included ferritin (an iron storage protein), mitochondrial iron (consisting primarily of Fe/S clusters and hemes), and mononuclear nonheme high-spin (NHHS) Fe^{II} and Fe^{III} species. Brains from prenatal and one-week old mice were dominated by ferritin and were deficient in mitochondrial Fe. During the next few weeks of life, the brain grew and experienced a burst of mitochondriogenesis. Overall brain Fe concentration and the concentration of ferritin declined during this burst phase, suggesting that the rate of Fe incorporation was insufficient to accommodate these changes. The slow rate of Fe import and export to/from the brain, relative to other organs, was verified by an isotopic labeling study. Iron levels and ferritin stores replenished in young adult mice. NHHS Fe^{II} species were observed in substantial levels in brains of several ages. A stable free-radical species that increased with age was observed by EPR spectroscopy. Brains from mice raised on an Fe-deficient diet showed depleted ferritin iron but normal mitochondrial iron levels.

Keywords

Transition metals; iron metabolism; labile iron pool; anemia; blood brain barrier; Fenton chemistry; fetal development; reactive oxygen species

Iron plays a major role in generating the chemical energy required for neurological activity, in that Fe/S clusters and heme groups are abundant in mitochondrial respiratory complexes.[1] This transition metal is found at the active sites of numerous metalloenzymes in the brain[2] and is required for myelin biosynthesis.[3] Over a billion people worldwide suffer from anemia[4], and Fe deficiency affects neonatal brain development and cell-mediated immunity.[5] An overabundance of Fe is also problematic, as certain forms of iron, particularly NHHS Fe^{II} complexes, promote Fenton chemistry that generates reactive oxygen species (ROS). The brain may be particularly sensitive to ROS damage because of its high rate of O_2 consumption[6] and limited ability of neuronal cells to be repaired or replaced.[7] Moreover, Fe accumulates with age and neurodegeneration.[8]

*To whom correspondence should be addressed., Phone: 979-845-0956., Fax: 979-845-4719. lindahl@chem.tamu.edu.

Iron traveling into the brain passes through the blood-brain barrier (BBB).[9] Fe^{III}-bound transferrin in the blood binds to receptors on the luminal side of the endothelial cells associated with this barrier.[10] Once inside neurons and other cells of the brain, a portion of the Fe is trafficked to mitochondria, where hemes and iron-sulfur clusters are assembled. Another portion is stored as ferritin, a spherically shaped protein complex with a hollow core into which large amounts of Fe can be deposited in the form of magnetically-interacting Fe^{III} oxyhydroxide material.[11] Ferritin helps regulate cytosolic Fe concentrations and sequester Fe that might otherwise generate ROS. Similar forms of Fe are found in hemosiderin[12], a degradation product of ferritin, nueromelanin[13], and perhaps mitochondrial ferritin.[14]

X-ray fluorescence[15], high-field magnetic resonance imaging[16] and high-resolution histological staining[17] have revealed an inhomogeneous spatial distribution of Fe in the brain. The globus pallidus, putamen, substantia nigra pars reticulata, red nucleus, cerebral dentate nucleus, the nucleus accumbens and portions of the hippocampus contain high concentrations of Fe; white matter and the cerebrospinal fluid contain lesser amounts. The distribution of brain Fe follows the distribution of ferritin whereas the distribution of transferrin is more homogeneous[18], reflecting the dominance of ferritin Fe in the brain.

These imaging methods provide excellent *spatial* resolution of brain Fe but their ability to resolve different *types* of Fe-containing species is limited. Mössbauer spectroscopy can distinguish different types of Fe[19], but it has barely been applied to the brain, perhaps due to the insensitivity of the technique, the low concentration of Fe in the brain, and the ability of Mossbauer to detect only ^{57}Fe (2% natural abundance).

We have used Mössbauer spectroscopy, in conjunction with EPR and UV-vis spectroscopies, and ICP-MS, to assess the Fe content of yeast mitochondria, vacuoles and whole cells.[20–22] Our objective in those studies was to evaluate the types and relative amounts of Fe present in these organelles and cells. In yeast, the two dominant Fe “traffic hubs” include vacuoles, which store Fe, and mitochondria, which use it to obtain cellular energy.

Here we apply the same methods to study the iron content of intact ^{57}Fe-enriched mouse brains. Previous Mössbauer studies of the brain have focused on particular Fe-rich subcomponents of unenriched human brains. These studies found that virtually all Fe in these regions consists of magnetically interacting, superparamagnetic ferric species, including ferritin and nueromelanin[8, 11–14]; curiously, mitochondrial Fe, e.g. Fe/S clusters and heme groups were not observed. This is difficult to rationalize, given the enormous role of mitochondria in brain function, and the substantial proportion of yeast Fe due to this organelle. We show here that, besides ferritin-like species, the brains of mice contain substantial amounts of Fe/S clusters, much of it arising from mitochondria. Also detected were nonheme high-spin (HS) Fe^{II} and Fe^{III} species. A portion of these mononuclear species may constitute the labile iron pool (LIP) and which may participate in ROS-generating reactions.

Experimental Procedures

Animal care and dissection

C57BL/6 mice were raised and manipulated in accordance with the TAMU Animal Care and Use committee (AUP 2011-223). Mice were housed in disposable plastic cages (Innovive Innocage Static Short) with all-plastic water bottles and plastic feeders with zinc electroplated reinforcements. Mice were fed Fe-deficient chow (Harlan Laboratories, Inc. Teklad ID #80396) supplemented as follows. For experiments involving ^{56}Fe or ^{57}Fe, the

chow was supplemented with 50 μg/g of either natural abundance Fe citrate or ^{57}Fe citrate (IsoFlex USA) prepared as described.[22] For each kg of chow, 22 mL of a 40 mM stock solution of Fe citrate (adjusted to pH 7) was added. The chow was further moistened with *ca.* 45 mL of double-distilled water containing 0.6 ng Fe/g water. The chow was compressed into pellets, heated at 100°C for 20 min, and then stored at −20°C in zip-locked plastic bags. Samples of the 7 batches of this chow examined contained an average of 33 ± 2 μg Fe/g chow as determined by ICP-MS.

Fe-deficient pups were born to a mother that was fed the Fe-sufficient diet until ~3 days prior to birth when her diet was switched to Fe-deficient (1.2 μg Fe/g chow). Fe-deficient animals received water that was house-distilled, deionized using ion-exchange columns (Thermo Scientific 09-034-3), and distilled again using a sub-boiling still (Savillex DST-1000). The resulting sub-boiling distilled water contained 0.02 ng Fe/g water.

Each cage contained *ca.* 200 g of synthetic bedding (Ketchum Omega Dry) with 1.5 μg ^{56}Fe/g. Nestlets (Ancare) that were included in the cages of pregnant females weighed ~ 10 g and contained 20 μg ^{56}Fe/g. Nitrile gloves were worn when mice, chow, water, bedding, etc. were handled. So-called "^{56}Fe-enriched" mice were treated equivalently but were raised on chow supplemented with natural-abundance Fe citrate.

Mice were euthanized by an IP injection of a solution that provided 3 mg ketamine and 0.5 mg xylazine per 20 g body wt. Immediately after breathing ceased and the heart stopped beating, animals were imported into a refrigerated (5 – 10° C) argon-atmosphere glove box (MBraun Labmaster) containing between 2 – 20 ppm O_2, where all dissections and tissue manipulations were performed. The "hands" of a pair of standard butyl rubber gloves on the box were cut off and replaced with tight-fitting surgical gloves using custom-designed plastic cuffs. The open end of each surgical glove was stretched over one end of a cuff and secured with two O-rings that fit into grooves on the cuff. The other end of the cuff was attached similarly to a butyl rubber glove, the other end of which was secured on the box glove port in standard fashion.

Unless noted otherwise, animals were perfused with Ringer's buffer (155 mM NaCl, 5 mM KCl, 2 mM $CaCl_2$, 1 mM $MgCl_2$, 2 mM NaH_2PO_4, 10 mM HEPES, 10 mM glucose, and ~10 U heparin/mL). A 27 gauge 1/2″ long stainless-steel needle was inserted into the left ventricle of the heart, and buffer was pumped at *ca.* 0.7 mL/min. After ~1 min, the descending aorta was severed, and pumping continued for an additional 1–2 min until blanching of the liver was evident. For some dissections, blood diluted with Ringer's buffer was collected.

Immediately after perfusion, brains and other organs were isolated by dissection using stainless steel and/or titanium instruments. The ^{57}Fe concentration of a 50 mL solution of Ringer's buffer into which the stainless steel instruments were immersed for 30 min increased by 190 nM. This is far longer than animals contacted the instruments. Thus, an insignificant amount of ^{57}Fe was leached from these instruments during dissections and none of the Fe-associated features observed in the spectra originated from them.

Densities

Masses of dissected brains were determined using an analytical balance (Toledo Mettler Model AB104) in the glove box. Volumes were measured using a 10 mL graduated cylinder into which a Delrin screen, supported by a thin plastic line, was submersed in buffer. Brains were submersed into the cylinder and the displaced volumes were measured. Densities were determined for 6 samples; an average value of 1.17 g/mL was obtained, similar to the reported value of 1.06 g/mL.[23] The latter value was used for all calculations.

Mössbauer Spectroscopy

Whole brains were anaerobically loaded into Delrin Mössbauer cups and frozen as described.[24] Low-field spectra were collected using a model MS4 WRC spectrometer (SEE Co, Edina MN). High-field (6 T) and low-field spectra were collected at 4.3 K using a model 12CNDT-6T spectrometer (SEE Co, Edina MN). Spectra were analyzed using WMOSS software (SEE Co, Edina MN). Parameters are reported relative to α-Fe foil at room temperature.

EPR and UV-visible spectroscopy

Following Mössbauer analysis, brains were transferred to disposable plastic 15 mL tubes containing an equal volume of Ringer buffer. Samples were homogenized for 1 min using a plastic rotary knife inserted into a tissue grinder (Omni TH). For EPR measurements, homogenates were packed (4,000×g, 10 min) and frozen in custom quartz tubes as described.[24] Spectra were collected on an X-band spectrometer (EMX, Bruker Biospin Corp., Billerica MA) with an Oxford Instruments ER910 cryostat. For UV-Vis measurements, samples were transferred to a 2 mm pathlength custom-designed quartz cuvette (NSG Precision Cells), sealed anaerobically with a septum. RT UV-vis spectra were collected on a Hitachi 4400U spectrophotometer with a head-on photomultiplier tube. Spectra were analyzed as described for specific heme *a*, heme *b*, and heme *c* content as described.[20]

The contributions of blood from the UV-vis spectra of brain homogenates were removed, based on the percentage contribution of deoxyhemoglobin present in corresponding Mössbauer spectra of the same brain sample. This percentage was multiplied by the concentration of Fe in the sample, affording the concentration of hemoglobin (typically ~ 20 μM). The UV-vis spectrum of 100-fold diluted blood was determined (Figure S5), as was the Fe concentration of undiluted blood (7.6 mM Fe). The spectral absorbance was scaled based on the ratios of Fe concentrations in blood *vs.* in the brain samples, and the scaled spectra were subtracted from the raw UV-vis spectra of the corresponding brain homogenate.

ICP-MS

Homogenized brain samples were transferred to plastic tubes containing 350 μL of concentrated trace-metal-grade nitric acid (Fisher). After overnight digestion at 90° C, samples were diluted with 6.5 mL of H_2O and analyzed by ICP-MS (Agilent model 7700x). The H_2O used was sub-boiling distilled as described above.

Results

^{57}Fe-enrichment

The concentration of Fe in the mouse brain was so low (Tables 1) that ^{57}Fe enrichment was required for Mössbauer studies. To evaluate enrichment rates, mice born to an ^{56}Fe-enriched mother were fed ^{57}Fe-supplemented chow immediately after weaning. Their brains enriched slowly such that only partial ^{57}Fe-enrichment was achieved after 58 wks on the ^{57}Fe-supplemented diet (Figure 1). Other organs, including liver, spleen, heart, and kidney enriched faster and to a greater extent than the brain, with the duodenum enriching fastest (Tables S1 – S3). The slow incorporation of ^{57}Fe into the brain was probably due to the blood-brain barrier.[9] Cu, Mn, Zn, Mo and P concentrations in these organs were also determined (Table S4 – S8).

The rate of Fe enrichment was biphasic, with the transition from fast to slow phase occurring 4–6 wks postpartum. During the fast-enrichment period, the total nanomoles

of ^{56}Fe in the brain declined rapidly while that of ^{57}Fe increased gradually (Figure 1). The overall concentration of Fe in the brain *declined* during the fast-enrichment phase, followed by a gradual recovery in the slow-enrichment phase. Brain mass increased rapidly during the fast-enrichment phase and slowed thereafter. The concentration of ^{57}Fe in the brain increased with each generation raised under ^{57}Fe-enrichment conditions, maximizing at ~ 80% after about 3 generations. Thus, Mossbauer spectra were typically collected from animals raised under ^{57}Fe-enrichment conditions for ≥ 2 generations.

Brains from three wk old mice

The low-temperature low-field Mossbauer spectrum of a 3-wk old brain exhibited 4 discernible features. A sextet typical of ferritin-bound Fe^{III} ions dominated (Figure 2A); the blue line is a simulation with $\delta = 0.5$ mm/s, $\Delta E_Q = -0.3$ mm/s and $\Gamma = 0.6$ mm/s. At 70 K, this feature collapsed into a doublet ($\delta = 0.5$ mm/s and $\Delta E_Q = 0.7$ mm/s) (Figure 2B), similar to the behavior of authentic ferritin.[25] The baseline of the 70 K spectrum did *not* reveal underlying features. When a 6 T field was applied at 4.3 K, the resulting pattern (Figure 2C) associated with this feature was again indistinguishable from that of ferritin. We conclude that this feature arises from ferritin, but other magnetically interacting Fe^{III} ions such as Fe-bound haemosiderin[25], neuromelanin[13] or mitochondrial ferritin[14] could have contributed.

Another major feature in the spectrum was a quadrupole doublet with $\delta = 0.45$ mm/s and $\Delta E_Q = 1.15$ mm/s; these values are typical of S = 0 $[Fe_4S_4]^{2+}$ clusters and low-spin Fe^{II} heme centers. At 6 T, the splitting pattern observed for this so-called *Central Doublet* (CD) was simulated (Figure 2C, purple line) confirming the expected diamagnetism. A doublet with identical parameters in spectra of isolated mitochondria from yeast[20] arises primarily from respiratory complexes, and so we assign the majority of the CD intensity in brain to mitochondrial respiratory complexes.

The spectrum also exhibited a quadrupole doublet with $\delta \sim 1.4$ mm/s, $\Delta E_Q \sim 3.3$ mm/s arising from one or more NHHS Fe^{II} species. This is simulated by the green line in Figure 2B. These parameters are typical of such complexes with 5 – 6 O/N donor ligands. Most evident in the 70 K spectrum was the doublet from HS Fe^{II} heme centers (Figure 2B, yellow line).

UV-vis spectra of corresponding brain homogenate (Figure 3D) revealed the Soret, α and β bands indicating reduced hemes. These features were similar to those of yeast mitochondria[20]; their concentrations were quantified and are listed in Table 1.

Low-temperature EPR spectra of packed 4-wk mouse brain homogenates (Figure 4) were virtually identical to those of a 3-wk old animal but were slightly more intense. The spectra exhibited overlapping signals in the g = 2 region. Resonances at g = 1.93 and 1.86 probably arose from the S = ½ $[Fe_2S_2]^{1+}$ cluster of succinate dehydrogenase and the reduced Rieske S = ½ $[Fe_2S_2]^{1+}$ cluster associated with cytochrome bc_1, respectively.[20] Also evident was an isotropic signal at g = 2.00, probably from an organic radical. The weak signal at g = 4.3 undoubtedly arose from mononuclear HS Fe^{III} species with rhombic symmetry. The origin of the derivative-like feature at g = 2.16 is uncertain. Spin quantifications are listed in Table 1.

Brains from iron-deficient mice

A pregnant ^{57}Fe-enriched mouse was switched to Fe-deficient chow 3 days prior to giving birth, and her offspring were euthanized 3 wks later at which time they displayed alopecia (Figure S3), an indicator of Fe-deficiency.[26] Also, the average Fe concentration in their livers (260 μM) was nearly 6-fold lower than in Fe-replete livers. Beard *et al.* found a 4-fold

decline of liver Fe in mice fed an Fe-deficient diet for 8 wks.[27] The average Fe concentration in their brains (Table 1) was also less than in Fe-sufficient brains, but the fold change was less dramatic. Mössbauer spectra (Figure 2D) exhibited less of the ferritin sextet relative to Fe-sufficient brains, while, unexpectedly, the CD (purple line) was *more* intense. Also surprisingly was that the *absolute* concentration of the CD Fe in these brains was slightly *higher* than that in comparable Fe-sufficient brains (75 μM *vs*. 55 μM). A minor NHHS Fe^{II} feature was evident (Figure 2D, green line). EPR and UV-vis spectra of Fe-deficient brains exhibited the same suite of signals and comparable intensities as were observed in spectra from brains of Fe-sufficient mice.

Prenatal brains

Prenatal mice could not be perfused, such that the quadrupole doublet due to hemoglobin in the corresponding Mössbauer spectra was more intense than in the 3-wk brain spectra. The exact position of the heme doublet (δ = 0.96 mm/s, ΔE_Q = 2.35 mm/s) was also shifted slightly relative to that in other spectra, due to the presence of *fetal* hemoglobin in prenatal brains.[28]

The average Fe concentration in the prenatal brains (Table 1) included a significant contribution from blood (~ 100 μM). Since the concentration of Fe in undiluted blood was 7.8 mM (Table S9), we calculate that ~ 1.3% of the dissected prenatal brain volume was occupied by blood. This underestimates the value in living animals, as some blood exited the tissue during dissection. Apart from the blood contribution, the Mössbauer spectrum of prenatal brains was dominated by the ferritin sextet, with only a minor percentage due to the CD (Figure 2E, Table 1) A NHHS Fe^{II} doublet was evident (arrow), with intensity comparable to that of the 3 wk brain spectrum. The UV-vis spectrum of prenatal brain homogenate (Figure 3A) was dominated by features due to fetal hemoglobin; other heme-based species (e.g. mitochondrial cytochromes) could not be discerned. Intensities of EPR signals from the prenatal brain homogenate were diminished relative to those in other spectra (Figure S4A). These results indicate that ***prenatal brains were deficient in mitochondria***, with most Fe present as ferritin or ferritin-like species.

Brains from mice at different ages

Mössbauer spectra of brains from mice of different ages (Figure 2, E – G, and Figure S1) showed an age-dependent *increase* in the percentages of the CD and a relative *decrease* in the ferritin-like sextet. This is indicated most reliably by the ferritin:CD intensity ratios (Table 1) which was highest for prenatal brains and lowest at 4 wks. Mössbauer spectra of the 24 and 58 wk brains exhibited age-dependent increases in the percentage of the ferritin-like sextet and decreases in the CD. UV-vis spectra also showed an age-dependent increase in cytochromes at early ages (Figure 3). EPR spectra exhibited increasing intensities of the signals in the g = 2 region (Figure S4), including features that likely originate from mitochondria. The radical signal at g = 2.00 also increased with age, while the g = 4.3 signal intensity was age-invariant.

Discussion

During the 150 year history of studying Fe in the brain, the vast majority of imaging studies have involved staining the brain with Fe chelators, e.g. using Perls' stain.[29] This gives useful, albeit qualitative, estimates of the distribution of Fe. Quantitative estimates of brain Fe concentrations have been obtained by analytical methods (e.g. AA and ICP). Since the mid 1980's, the distribution of brain Fe has been monitored indirectly using NMR spectroscopy.[30] With this technique, Fe is detected indirectly, in that ferritin and other magnetic forms of Fe shorten T_2 relaxation times.[31] Magnetic susceptibility contrast

measurements have also been used as a reporter of brain Fe in MRI studies.[32] These are very powerful techniques, but they also have limitations. They can only detect magnetic forms of Fe, such that diamagnetic Fe are not detected. Non-iron paramagnetic metal ions will also affect NMR-based measurements, which complicate analyses.[33]

X-ray absorption spectroscopy does not suffer from these problems, and has also been used to evaluate the spatial distribution of brain Fe.[33, 34] This method measures Fe directly, regardless of magnetic properties, and has some ability to distinguish oxidation states. XAS methods have shown that the brain contains both Fe^{II} and Fe^{III} ions, with the Fe^{III} state dominating.[34] Wang et al.[35] and Pushie et al.[15] used synchrotron X-ray fluorescence spectroscopy to map the distribution of Fe and other metals in the mouse brain. However, the type of Fe centers, including oxidation states and coordination environments, could not be determined.

Mössbauer spectroscopy can play a complementary role to these other spectroscopic method, as it has unique strengths and weaknesses. The low-sensitivity of standard Mössbauer spectroscopy precludes its use in spatially resolving brain Fe, and the requirement for ^{57}Fe-enrichment limits the technique (for practical reasons) to the study of rodent brains. Although it might be possible to study micro-dissected regions of a mouse or rat brain, this would take many animals and thus we have focused in this initial study on whole intact mouse brains. Thus, our results reflect the *average of all of the ^{57}Fe nuclei distributed inside the brain, without any spatial resolution*. Mössbauer spectroscopy also has distinct and powerful advantages, relative to these other spectroscopic methods, in its ability to resolve different types of Fe centers in the brain and to determine, with great precision, the percentage of each type of Fe present. No other method can compete with Mössbauer spectroscopy in this regard.

Comparison to Previous Mössbauer Studies

The only type of Fe observed in previous Mössbauer studies of the brain was a sextet due to ferritin or ferritin-like Fe.[11,36,37] The Mössbauer spectra presented here are *significantly* different in that other types of Fe were observed. Why none of the previously published spectra of brain displayed the CD, a heme quadrupole doublet, or NHHS Fe^{II} species is puzzling but perhaps rationalize-able. Previous studies utilized human brains which were unenriched in ^{57}Fe; this diminished the spectral quality greatly such that minor species, e.g. NHHS Fe^{II}, could have gone undetected. That does not explain why intense features, like those originating from heme centers or the CD, would not have been observed. We suspect that blood would have been drained from postmortem human samples, explaining the absence of spectral features due to hemoglobin. Previous spectra were exclusively obtained on Fe-rich regions of the brain (e.g. the substantia nigra), which may be dominated by ferritin Fe. The averaged Fe content of the entire brain may not be dominated by ferritin to this extent. More speculatively, the human donors were generally at the end of their natural lifespan, and older brains may possibly contain more ferritin than younger and middle-aged ones, the age periods we have studied here.[38] Finally, the concentration of Fe in the average human diet may be higher, relatively speaking, than in our mouse chow, which could translate into relatively more ferritin and less CD in the human brain. Further studies are required to examine each of these possibilities.

Incorporation of Fe into Brain

In this study, we found that young mouse brains exchanged Fe rapidly during the rapid growth phase, including the *export* of Fe. This resulted in an overall *decline* in the concentration of Fe in the brain. During this period, the brain appears to grow faster than could be maintained by the rate of Fe import, such that ferritin stores were activated. With

age, the dynamic exchange of Fe slows, brain growth slows, and the concentration of Fe in the brain recovers. During the first month of life, the proportion of stored Fe declines while the proportion of mitochondrial Fe increases. As the animals become adults, the proportion of stored Fe increases again. In our study, the concentration of mitochondria did not decline noticeably up to 58 wks; we are currently investigating whether mitochondrial levels decline towards the end of the animal's natural lifespan, as has been reported.[7]

A decline of Fe concentration in the brain immediately after birth has been reported.[39–41] Keen and Hurley measured age-dependent brain Fe concentrations in hybrid mice.[39] At birth, Fe concentrations were 17.3 μg Fe/gm brain wet wt (which corresponds to 330 μM using the same density assumed here). By days 5 – 8, the brain contained 8.6 μg Fe/gm (160μM). By day 60, [Fe] returned to newborn levels.

Burst of Mitochondriogenesis

In yeast cells, the Mössbauer CD and HS heme doublet, the g = 1.94 and 1.90 EPR signals and the heme *a*, *b*, and *c* UV-vis signals arise primarily from the mitochondrial respiratory complexes[20], and so we have assigned the analogous features in brain spectra similarly. The intensity of these signals, considered collectively, undoubtedly reflects the concentration of mitochondria in the brain. The ferritin-like sextet in the Mössbauer spectrum reflects brain Fe that is stored. These assignments are supported by a recent study of the ironome of human Jurkat cells and their isolated mitochondria.[42]

Our results show that most of the Fe in the brain of prenatal and newborn mice is stored, and that during the first month of life, the proportion of stored Fe declines while the proportion of mitochondrial Fe increases. As the animals move into adulthood, the proportion of stored Fe in the brain increases again. We did not detect an overall decline in the concentration of mitochondria with age up to 58 wks; further studies are underway to determine whether mitochondrial levels decline towards the end of the animal's natural lifespan. Mitochondrial levels have been reported to decline with age due to mitophagy.[7]

These results, in conjunction with those of the ^{57}Fe incorporation study, suggest a connection between this burst of mitochondriogenesis and an increase in brain activity (Figure 5). Before birth and immediately thereafter, the level of brain activity is low and so might be the demand for energy. During this period, Fe is slowly imported into the brain where most of it is stored as ferritin or ferritin-like material. During the first few weeks of life, there is an increased level of brain activity as the animal's eyes open and they explore their environment. The increased brain activity increases the demand for more chemical energy, prompting a burst of mitochondriogenesis. This demand for Fe is beyond that at which Fe can be imported into the brain. Thus, the brain draws upon its Fe stores to build the requisite Fe/S clusters and heme centers. The scarcity of Fe is exacerbated by the rapid increase of brain volume during the same period, resulting in the overall decline in the Fe concentration in the brain. Eventually, the burst of mitochondriogenesis slows, as does the rate of brain growth. The brain replenishes its Fe stores, via the slow import of Fe from the blood, and it reestablishes a higher overall Fe concentration.

This model is consistent with previous results. Pysh and co-workers used electron microscopy to determine the proportion of rat cell volume (in the inferior colliculus) due to mitochondria during different stages of development.[43] The mitochondrial profile number was relatively low during the first few postnatal days but increased rapidly thereafter, leveling off at *ca*. 25 days postnatal. The mitochondrial volume fraction increased 6-fold, reaching 9% of tissue volume in adults. Interestingly, there was no correlation of mitochondria with synapse *concentrations*; rather, the rate of mitochondriogenesis correlated with increased levels of synaptic *activity*.

Effect of Iron deficiency

Our results indicate that the regulation of brain Fe is sensitive to dietary changes. The brain responds to Fe deficiency by reducing levels of stored ferritin Fe while maintaining normal mitochondria levels. Ten-day old rats fed an Fe-deficient diet for 28 days showed a 27% decline in non-heme brain Fe[44], similar to the 25% decline that we observed. Interestingly, in our study, the concentration of mitochondria in Fe-deficient brains was actually *higher* than observed in Fe-sufficient animals at any developmental stage examined. Explaining this counterintuitive result will require further study, but Fe regulation in the brain is undoubtedly complex, and the brain is probably protected from organism-level Fe deficiencies. In other studies, levels of the brain Fe-containing proteins tyrosine hydroxlase, tryptophan hydroxylase, monoamine oxidase, succinate hydroxylase and cytochrome *c* in Fe deficient animals were also normal.[45] Mackler *et al*.[46] reported that the levels of cytochromes *a* and *c* were normal under Fe deficient conditions, and that that the level of cytochrome *b* was only slightly reduced relative to in Fe-sufficient mitochondria. Neurological problems may only arise if the Fe deficiency is so severe that all storage forms of Fe in the animal have been exhausted and the brain can no longer be protected from the deficiency.

Mononuclear Nonheme high-spin Ferrous and Ferric Species

Our results indicate the presence of substantial amounts of NHHS Fe^{II} in the mouse brain. NHHS Fe^{II} complexes are generally less tightly coordinated than LS complexes and they exhibit more rapid ligand-exchange. Such properties would be expected for trafficking Fe and for complexes that undergo Fenton chemistry. Three of our Mössbauer spectra clearly indicate the presence of substantial concentrations of NHHS Fe^{II} species in the brain (−1 wk, 3 wks, and Fe-deficient). In these cases, the concentration of all NHHS Fe^{II} species in the mouse brain was ~ 20 μM. The NHHS Fe^{II} doublets were broad, suggesting that many NHHS Fe^{II} species contribute. The NHHS Fe^{II} doublet in the other brain Mössbauer spectra were present but less well resolved.

The g = 4.3 EPR signal was present in every brain homogenate examined; this indicates the presence of HS Fe^{III} ions with rhombic symmetry in the brain. The quantified intensity of this signal indicates that these Fe^{III} species are present at a combined concentration of ~ 100 nM. A portion of these species are undoubtedly Fe^{II} and Fe^{III} ions bound tightly in the active site of enzymes in the brain; perhaps some is present as Fe^{III} transferrin.[47] Another portion may be involved in trafficking and/or the Labile Iron Pool (LIP).[48–50] Such species have not been observed in previous Mössbauer and EPR studies of the brain.[51–53]

Other groups have reported the presence “chelatable”, “free, “labile” or “loosely-bound Fe in the brain. These pools of Fe are defined operationally, i.e. as the Fe in supernatant fractions of brain extracts treated with Fe chelators and then spun by centrifugation. Sohal *et al*.[54] measured bleomycin-chelated and ferrozine-chelated (called nonheme) Fe in the mouse brain, and observed an age-dependent increase of nonheme Fe but not bleomycin-chelatable Fe. Magaki *et al*.[55] measured “loosely bound iron” and “non-heme iron”, defined operationally, in 6, 12, and 24 week old mouse brains. They found that loosely bound Fe represented 20% – 30% of non-heme Fe, with the latter type of Fe increasing with age and the former decreasing slightly or remaining constant. Using chelator induced calcein-quenching, Kaur et al.[56] found that an operationally defined LIP in mouse brain increased with age. Other LIPs are defined by staining the brain directly. Using high-resolution histological staining methods, Meguro *et al*.[17] reported substantial amounts of (again, operationally defined) nonheme Fe^{II} and Fe^{III} species distributed heterogeneously throughout the rat brain. They determined that the levels of these species increase with the age of the animal.

All of these previously reported LIPs, defined by their chelation ability, differ fundamentally from the mononuclear HS Fe^{II} and Fe^{III} species observed here. The species we observed are defined solely by their spectroscopic properties, not by their chelation properties. Comparing the two will require establishing the chelation properties of the species we observe and the spectroscopic properties of the chelatable Fe species reported previously.

Spin radical species

The radical species detected here may be physiologically relevant since samples were prepared in the absence of O_2 which minimizes the possibility of generating artifactual radical signals during sample preparation. Transient radicals in the brain have been detected using spin-probes[57] but the radical detected here is fundamentally different because it is stable in the absence of such probes (radical probes trap unstable radicals). Radical species are cleared from the brain faster in young mice than in old, suggesting that the reducing capacity of the brain may decrease with age.[58] These changes may be related to the age-dependent increase in the stable radical species that we observed by EPR. Most theories of aging involve the age-dependent accumulation of ROS[59], which could be responsible for the gradual build-up of the stable radical.

Conclusions

Our study provides new insights into Fe metabolism, trafficking and homeostasis in the brain. We have enriched mice with ^{57}Fe and have used Mössbauer spectroscopy, along with EPR, UV-vis and ICP-MS, as biophysical probes of the types of Fe centers contained in the mouse brain at different stages of development. We quantified the rates of Fe incorporation into the brain, and found that Fe is imported slowly, relative to the rate of import into other organs. The slow rate of Fe incorporation into the brain is probably due to the tight regulation at the BBB. The rate of Fe incorporation is biphasic, with a rapid phase occurring in very young animals and a slower phase occurring in adult animals. During the rapid Fe-incorporation phase, the brain grows rapidly, and the level of brain activity increases. As such, ATP-generating mitochondria are being generated rapidly. This creates a high demand for Fe. This demand cannot be met solely with newly imported Fe. As a result, the concentration of Fe in the brain declines and some ferritin-stored Fe is released and used for mitochondriogenesis. As brain growth and mitochondriogenesis slow, the Fe import rate becomes sufficient to allow some of the imported Fe to be stored once again.

The brain contains substantial concentrations of NHHS Fe^{II} and Fe^{III} species a portion of which may be used in trafficking and homeostasis. Iron in this category is known to undergo the Fenton reaction to generate reactive oxygen species which is associated with aging. Further studies are required to determine whether the detected Fe species actually participate in such reactions. We observed a stable organic radical EPR signal which increased with age, consistent with the ROS theory of aging. Only ferritin-like Fe was observed in previous Mössbauer studies of the human brain, possibly because only Fe-rich regions were examined, and/or because of differences in the age and/or diets of the mice vs. human involved. We demonstrated that the Fe content of the brain is sensitive to diet, in that stored Fe was preferentially utilized when mice were Fe-deficient.

The methods developed here are widely applicable, and could be applied to any and all mouse organs, including those found in transgenic animals with various Fe-associated disorders. This approach may reveal differences in Fe metabolism, trafficking and/or regulatory homeostasis, and thus significantly impact the mechanistic study of Fe-related diseases.

Supplementary Material

Refer to Web version on PubMed Central for supplementary material.

Acknowledgments

The National Institutes of Health (GM084266) and the Robert A Welch Foundation (A1170) sponsored this study.

Abbreviations

LIP	labile iron pool
ICP-MS	inductively coupled plasma mass spectrometry
ROS	reactive oxygen species
BBB	blood brain barrier
EPR	electron paramagnetic resonance
HS	high-spin
LS	low spin
CD	central doublet
NHHS	nonheme high-spin

References

1. Greenamyre JT, Horowitz MP. Mitochondrial Iron Metabolism and Its Role in Neurodegeneration. J Alzheimers Dis. 2010; 20:S551–S568. [PubMed: 20463401]
2. Fitzpatrick PF. Tetrahydropterin-dependent amino acid hydroxylases. Annu Rev Biochem. 1999; 68:355–381. [PubMed: 10872454]
3. Ortiz E, Pasquini JM, Thompson K, Felt B, Butkus G, Beard J, Connor JR. Effect of manipulation of iron storage, transport, or availability on myelin composition and brain iron content in three different animal models. J Neurosci Res. 2004; 77:681–689. [PubMed: 15352214]
4. Ramakrishnan U, Rivera J, Villalpando S, Gonzalez-Cossio T, Martorell R, Neufeld LM. Prevalence of anemia and iron deficiency during pregnancy of women supplemented with iron or iron and multiple micronutrients. Faseb Journal. 2001; 15:A641–A641.
5. Beard J, Erikson KM, Jones BC. Neonatal iron deficiency results in irreversible changes in dopamine function in rats. Journal of Nutrition. 2003; 133:1174–1179. [PubMed: 12672939]
6. Halliwell B. Oxidative stress and neurodegeneration: where are we now? J Neurochem. 2006; 97:1634–1658. [PubMed: 16805774]
7. Green DR, Galluzzi L, Kroemer G. Mitochondria and the autophagy-inflammation-cell death axis in organismal aging. Science. 2011; 333:1109–1112. [PubMed: 21868666]
8. Gerlach M, Ben-Shachar D, Riederer P, Youdim MB. Altered brain metabolism of iron as a cause of neurodegenerative diseases? J Neurochem. 1994; 63:793–807. [PubMed: 7519659]
9. Wu LJ, Leenders AG, Cooperman S, Meyron-Holtz E, Smith S, Land W, Tsai RY, Berger UV, Sheng ZH, Rouault TA. Expression of the iron transporter ferroportin in synaptic vesicles and the blood-brain barrier. Brain Res. 2004; 1001:108–117. [PubMed: 14972659]
10. Fishman JB, Rubin JB, Handrahan JV, Connor JR, Fine RE. Receptor-mediated transcytosis of transferrin across the blood-brain barrier. J Neurosci Res. 1987; 18:299–304. [PubMed: 3694713]
11. Zecca L, Gallorini M, Schunemann V, Trautwein AX, Gerlach M, Riederer P, Vezzoni P, Tampellini D. Iron, neuromelanin and ferritin content in the substantia nigra of normal subjects at different ages: consequences for iron storage and neurodegenerative processes. J Neurochem. 2001; 76:1766–1773. [PubMed: 11259494]

12. Bell SH, Weir MP, Dickson DP, Gibson JF, Sharp GA, Peters TJ. Mössbauer spectroscopic studies of human haemosiderin and ferritin. Biochimica Et Biophysica Acta. 1984; 787:227–236. [PubMed: 6733119]
13. Gerlach M, Trautwein AX, Zecca L, Youdim MB, Riederer P. Mössbauer spectroscopic studies of purified human neuromelanin isolated from the substantia nigra. J Neurochem. 1995; 65:923–926. [PubMed: 7616255]
14. Bou-Abdallah F, Santambrogio P, Levi S, Arosio P, Chasteen ND. Unique iron binding and oxidation properties of human mitochondrial ferritin: a comparative analysis with Human H-chain ferritin. J Mol Biol. 2005; 347:543–554. [PubMed: 15755449]
15. Pushie MJ, Pickering IJ, Martin GR, Tsutsui S, Jirik FR, George GN. Prion protein expression level alters regional copper, iron and zinc content in the mouse brain. Metallomics. 2011; 3:206–214. [PubMed: 21264406]
16. Rodrigue KM, Haacke EM, Raz N. Differential effects of age and history of hypertension on regional brain volumes and iron. Neuroimage. 2011; 54:750–759. [PubMed: 20923707]
17. Meguro R, Asano Y, Odagiri S, Li C, Shoumura K. Cellular and subcellular localizations of nonheme ferric and ferrous iron in the rat brain: a light and electron microscopic study by the perfusion-Perls and -Turnbull methods. Arch Histol Cytol. 2008; 71:205–222. [PubMed: 19359804]
18. Connor JR, Menzies SL, St Martin SM, Mufson EJ. A histochemical study of iron, transferrin, and ferritin in Alzheimer's diseased brains. J Neurosci Res. 1992; 31:75–83. [PubMed: 1613823]
19. Glaser, T. Mössbauer Spectroscopy and Transition Metal Chemistry. Fundamentals and Applications. In: Gütlich, Philipp; Bill, Eckhard; Trautwein, Alfred X., editors. Angewandte Chemie International Edition. Vol. 50. 2011. p. 10019-10020.
20. Garber Morales J, Holmes-Hampton GP, Miao R, Guo Y, Münck E, Lindahl PA. Biophysical characterization of iron in mitochondria isolated from respiring and fermenting yeast. Biochemistry. 2010; 49:5436–5444. [PubMed: 20536189]
21. Holmes-Hampton GP, Miao R, Morales JG, Guo YS, Münck E, Lindahl PA. A Nonheme High-Spin Ferrous Pool in Mitochondria Isolated from Fermenting Saccharomyces cerevisiae. Biochemistry. 2010; 49:4227–4234. [PubMed: 20408527]
22. Cockrell AL, Holmes-Hampton GP, McCormick SP, Chakrabarti M, Lindahl PA. Mössbauer and EPR Study of Iron in Vacuoles from Fermenting Saccharomyces cerevisiae. Biochemistry. 2011; 50:10275–10283. [PubMed: 22047049]
23. Boutaleb S, Pouget JP, Hindorf C, Pelegrin A, Barbet J, Kotzki PO, Bardies M. Impact of Mouse Model on Preclinical Dosimetry in Targeted Radionuclide Therapy. Proceedings of the IEEE. 2009; 97:2076–2085.
24. Lindahl PA, Morales JG, Miao R, Holmes-Hampton G. Isolation of *Saccharomyces Cerevisiae* Mitochondria for Mössbauer, EPR, and Electronic Absorption Spectroscopic Analyses. Method Enzymol. 2009; 456:267–285.
25. Bell SH, Weir MP, Dickson DP, Gibson JF, Sharp GA, Peters TJ. Mössbauer spectroscopic studies of human haemosiderin and ferritin. Biochim Biophys Acta. 1984; 787:227–236. [PubMed: 6733119]
26. Vanderford DA, Greer PK, Sharp JM, Chichlowski M, Rouse DC, Selim MA, Hale LP. Alopecia in IL-10-deficient mouse pups is c-kit-dependent and can be triggered by iron deficiency. Exp Dermatol. 2010; 19:518–526. [PubMed: 20100190]
27. Beard JL, Wiesinger JA, Li N, Connor JR. Brain iron uptake in hypotransferrinemic mice: influence of systemic iron status. J Neurosci Res. 2005; 79:254–261. [PubMed: 15578731]
28. Oshtrakh MI. The features of Mössbauer spectra of hemoglobin in relation to the quadrupole splitting and heme iron stereochemistry. Z Naturforsch A. 1998; 53:608–614.
29. Koeppen AH. A brief history of brain iron research. J Neurol Sci. 2003; 207:95–97. [PubMed: 12614937]
30. Drayer B, Burger P, Darwin R, Riederer S, Herfkens R, Johnson GA. Magnetic-Resonance-Imaging of Brain Iron. Am J Neuroradiol. 1986; 7:373–380.
31. Wansapura JP, Holland SK, Dunn RS, Ball WS. NMR relaxation times in the human brain at 3.0 tesla. Jmri-J Magn Reson Im. 1999; 9:531–538.

32. Yao B, Li TQ, van Gelderen P, Shmueli K, de Zwart JA, Duyn JH. Susceptibility contrast in high field MRI of human brain as a function of tissue iron content. Neuroimage. 2009; 44:1259–1266. [PubMed: 19027861]
33. Hopp K, Popescu BFG, McCrea RPE, Harder SL, Robinson CA, Haacke ME, Rajput AH, Rajput A, Nichol H. Brain Iron Detected by SWI High Pass Filtered Phase Calibrated with Synchrotron X-Ray Fluorescence. J Magn Reson Imaging. 2010; 31:1346–1354. [PubMed: 20512886]
34. Szczerbowska-Boruchowska M, Lankosz M, Czyzycki M, Adamek D. An integrated experimental and analytical approach to the chemical state imaging of iron in brain gliomas using X-ray absorption near edge structure spectroscopy. Anal Chim Acta. 2011; 699:153–160. [PubMed: 21704769]
35. Wang H, Wang M, Wang B, Li M, Chen H, Yu X, Zhao Y, Feng W, Chai Z. The distribution profile and oxidation states of biometals in APP transgenic mouse brain: dyshomeostasis with age and as a function of the development of Alzheimer's disease. Metallomics. 2012; 4:289–296. [PubMed: 22301945]
36. Dubiel SM, Zablotna-Rypien B, Mackey JB. Magnetic properties of human liver and brain ferritin. Eur Biophys J. 1999; 28:263–267. [PubMed: 10192938]
37. Galazka-Friedman J, Bauminger ER, Friedman A, Barcikowska M, Hechel D, Nowik I. Iron in parkinsonian and control substantia nigra- a Mössbauer spectroscopy study. Mov Disord. 1996; 11:8–16. [PubMed: 8771061]
38. Bartzokis G, Tishler TA, Shin IS, Lu PH, Cummings JL. Brain ferritin iron as a risk factor for age at onset in neurodegenerative diseases. Annals of the New York Academy of Sciences. 2004; 1012:224–236. [PubMed: 15105269]
39. Keen CL, Hurley LS. Developmental changes in concentrations of iron, copper, and zinc in mouse tissues. Mech Ageing Dev. 1980; 13:161–176. [PubMed: 7432004]
40. Moos T, Morgan EH. Transferrin and transferrin receptor function in brain barrier systems. Cell Mol Neurobiol. 2000; 20:77–95. [PubMed: 10690503]
41. Connor JR, Menzies SL, Burdo JR, Boyer PJ. Iron and iron management proteins in neurobiology. Pediatr Neurol. 2001; 25:118–129. [PubMed: 11551742]
42. Jhurry ND, Chakrabarti M, McCormick SP, Holmes-Hampton GP, Lindahl PA. Ironome of Human Jurkat Cells and Isolated Mitochondria. 2012 Submitted to Biochemistry (bi-2012-00382d).
43. Pysh JJ. Mitochondrial changes in rat inferior colliculus during postnatal development: an electron microscopic study. Brain Res. 1970; 18:325–342. [PubMed: 5511217]
44. Dallman PR, Siimes MA, Manies EC. Brain iron: persistent deficiency following short-term iron deprivation in the young rat. Br J Haematol. 1975; 31:209–215. [PubMed: 1201239]
45. Ashkenazi R, Ben-Shachar D, Youdim MB. Nutritional iron and dopamine binding sites in the rat brain. Pharmacol Biochem Behav. 1982; 17(Suppl 1):43–47. [PubMed: 7184034]
46. Mackler B, Person R, Grace R. Iron deficiency in the rat: effects on energy metabolism in brown adipose tissue. Pediatr Res. 1985; 19:989–991. [PubMed: 4058979]
47. Price ME, Gibson JF. A re-interpretation of bicarbonate-free ferric transferrin E.P.R. spectra. Biochem Bioph Res Co. 1972; 46:646–651.
48. Tangeras A, Flatmark T, Backstrom D, Ehrenberg A. Mitochondrial Iron Not Bound in Heme and Iron-Sulfur Centers - Estimation, Compartmentation and Redox State. Biochimica Et Biophysica Acta. 1980; 589:162–175. [PubMed: 6243966]
49. Rauen U, Petrat F, de Groot H. Determination of the chelatable iron pool of isolated rat hepatocytes by digital fluorescence microscopy using the fluorescent probe, phen green SK. Hepatology. 1999; 29:1171–1179. [PubMed: 10094962]
50. Rauen U, Petrat F, de Groot H. Subcellular distribution of chelatable iron: a laser scanning microscopic study in isolated hepatocytes and liver endothelial cells. Biochemical Journal. 2001; 356:61–69. [PubMed: 11336636]
51. Wypijewska A, Galazka-Friedman J, Bauminger ER, Wszolek ZK, Schweitzer KJ, Dickson DW, Jaklewicz A, Elbaum D, Friedman A. Iron and reactive oxygen species activity in parkinsonian substantia nigra. Parkinsonism Relat Disord. 2010; 16:329–333. [PubMed: 20219408]
52. Friedman A, Arosio P, Finazzi D, Koziorowski D, Galazka-Friedman J. Ferritin as an important player in neurodegeneration. Parkinsonism Relat Disord. 2011; 17:423–430. [PubMed: 21550835]

53. Galazka-Friedman, J. Iron as a risk factor in neurological diseases ICAME 2007. Gajbhiye, NS.; Date, SK., editors. Springer; Berlin Heidelberg: 2009. p. 31-44.

54. Sohal RS, Wennberg-Kirch E, Jaiswal K, Kwong LK, Forster MJ. Effect of age and caloric restriction on bleomycin-chelatable and nonheme iron in different tissues of C57BL/6 mice. Free Radic Biol Med. 1999; 27:287–293. [PubMed: 10468200]

55. Magaki S, Mueller C, Yellon SM, Fox J, Kim J, Snissarenko E, Chin V, Ghosh MC, Kirsch WM. Regional dissection and determination of loosely bound and non-heme iron in the developing mouse brain. Brain Res. 2007; 1158:144–150. [PubMed: 17560557]

56. Kaur D, Rajagopalan S, Andersen JK. Chronic expression of H-ferritin in dopaminergic midbrain neurons results in an age-related expansion of the labile iron pool and subsequent neurodegeneration: implications for Parkinson's disease. Brain Res. 2009; 1297:17–22. [PubMed: 19699718]

57. Sano H, Naruse M, Matsumoto K, Oi T, Utsumi H. A new nitroxyl-probe with high retention in the brain and its application for brain imaging. Free Radic Biol Med. 2000; 28:959–969. [PubMed: 10802228]

58. Gomi F, Utsumi H, Hamada A, Matsuo M. Aging retards spin clearance from mouse brain and food restriction prevents its age-dependent retardation. Life Sci. 1993; 52:2027–2033. [PubMed: 8388983]

59. Cadenas E, Davies KJ. Mitochondrial free radical generation, oxidative stress, and aging. Free Radic Biol Med. 2000; 29:222–230. [PubMed: 11035250]

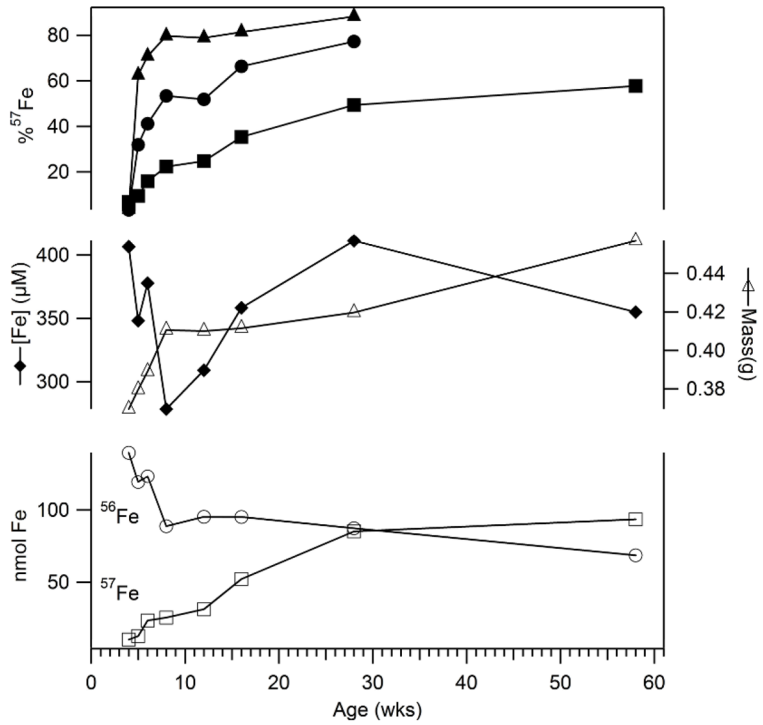

Figure 1. Enrichment of ^{57}Fe into ^{56}Fe-enriched mice

Upper plots refer to the % ^{57}Fe scale, including solid triangles (duodenum), circles (average of liver, kidney, heart and spleen) and squares (brain). Solid diamonds in the middle plots refer to total [Fe] in the brain; open triangles refer to brain mass. In the lower plots, open circles and squares refer to nmoles of ^{56}Fe and ^{57}Fe in the brain, respectively. Individual values and statistics are in Tables S1–S3.

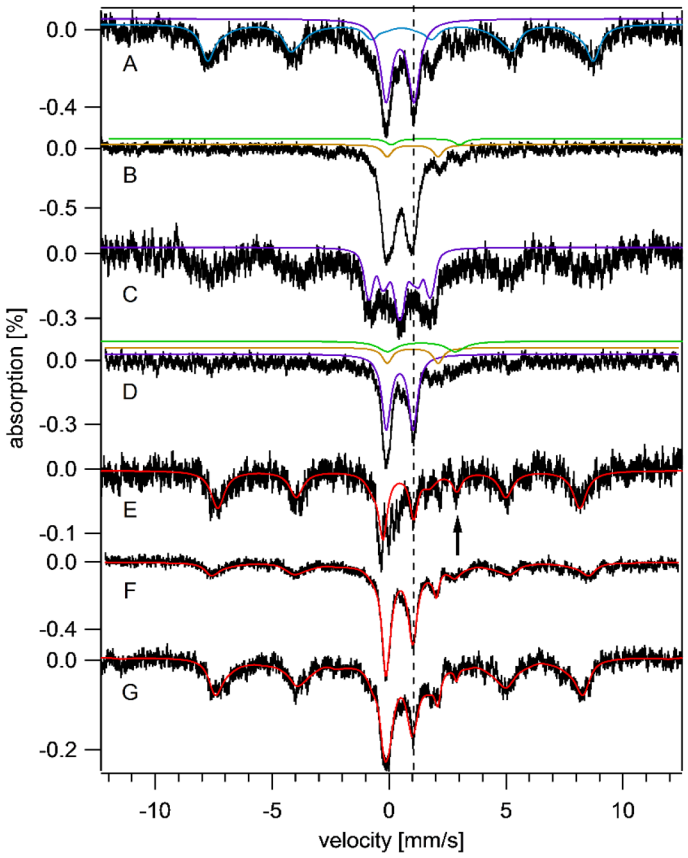

Figure 2. Mössbauer spectra of brains isolated at different ages

Spectra were collected at 6 K and with a 0.05 T field applied parallel to the radiation unless otherwise noted. **A**, 3 wk brain; **B**, same as **A** but at 70 K; **C**, same as **A** but at 4.3 K and 6 T field applied perpendicular to the radiation; **D**, 3wk Fe-deficient brain; **E,** −1wk brain; **F,** 4 wk brain; **G,** 58 wk brain. Red lines are composite simulations for **E** – **G.** Simulations assumed parameters mentioned in the text and percentages in Table 1. The vertical dashed line shows the position of the high-energy line of the central doublet. The arrow in **E** shows the position of the NHHS Fe^{II} feature. H_{int} values associated with the ferritin sextet ranged from 480 – 506 kG, perhaps reflecting subtle differences in the ferritin core structure.

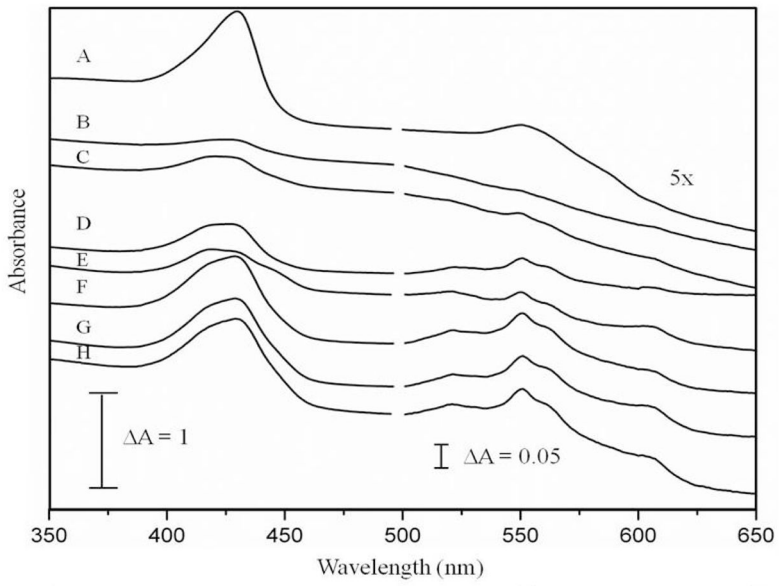

Figure 3. UV-vis spectra of brains isolated at different ages

A, −1 wk; **B**, 1 wk; **C**, 2 wks; **D**, 3 wks; **E**, 3 wks and Fe-deficient; **F**, 4 wks; **G**, 24 wks; and **H**, 58 wks. Intensities at wavelengths > 500 nm were multiplied by 5. Contributions due to hemoglobin have not been removed in the displayed spectra.

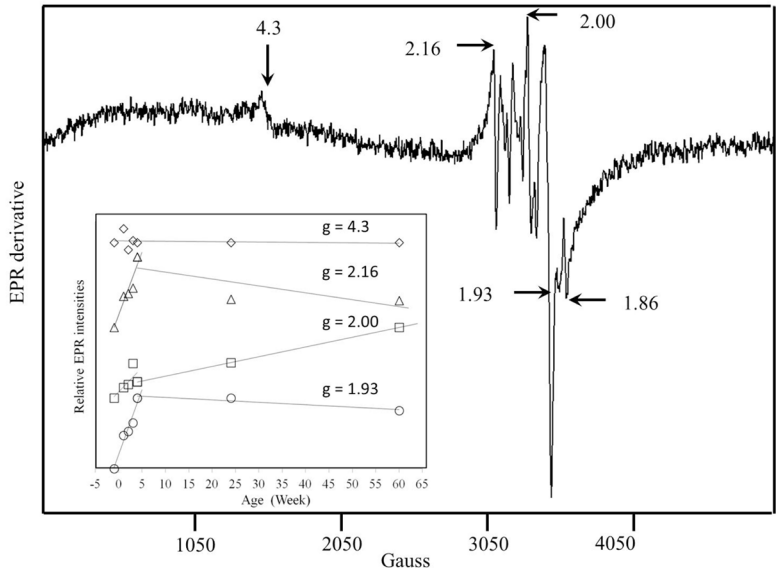

Figure 4. EPR spectrum of 4 wk brains

Highlighted EPR signals in the bottom panel are indicated by arrows. Conditions: temperature, 4 K; microwave frequency, 9.43 GHz; microwave power, 0.2 mW; modulation amplitude, 10 G; sweep time, 335 sec; time constant, 164 msec. The average of 10 scans is shown. Spectra of brains isolated from animals at other ages are given in Fig. S4. The inset shows the relative intensity of highlighted features as a function of age. Plots are offset by arbitrary amounts.

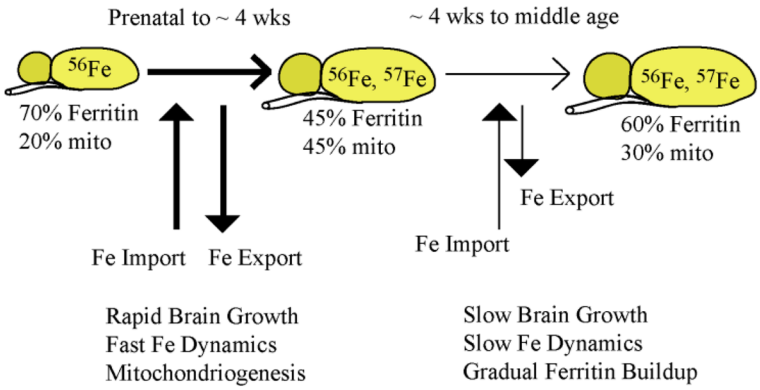

Figure 5. Model of Fe utilization in the developing mouse brain

During the first ~ 4 wks of life, the mouse brain grows rapidly and exhibits a rapid dynamic exchange of Fe with the blood, including both import and export of Fe to/from the brain. Early during this period most of the Fe in the brain is present as ferritin or ferritin-like material. During the first week or so of life, brain growth and mitochondriogenesis are so fast that Fe cannot be imported rapidly enough to maintain the overall [Fe] in the brain. The decline in [Fe] within neuronal cells causes some ferritin-like Fe to be released, with much of that Fe used for mitochondriogenesis. Gradually, the [Fe] in the brain recovers, rates of dynamic Fe import/export slow, and a greater proportion of Fe becomes stored as ferritin.

Table 1

Summary of Results. The concentration of heme *b* in the prenatal brain (*) was not quantified. Values obtained by EPR, UV-vis, ICP-MS and protein analyses have an estimated relative uncertainty of ± 20%. Values derived from Mössbauer analyses have an absolute estimated uncertainty of ± 4%.

Age (wks)	**−1**	**1**	**2**	**3**	**3**	**4**	**24**	**58**
Comments	Not Perfused				Iron Deficient			
Number and Sex	6 (sex not determined)	7F 2M	1F 2M	0F 3M	1F 8M	1F 3M	0F 2M	0F 1M
Average brain mass (mg)	52 ± 6	200 ± 30	350 ± 4	310 ± 40	350 ± 10	390 ± 30	377 ± 2	456
Num. used for element, protein analysis	6	4	2	3	3	2	2	1
[Protein] (mg/mL)	21	30	29	40	32	40	28	33
[Cu] (μM)	21	6	2	1	20	5	17	26
[Mn] (μM)	21	3	6	6	26	11	5	6
[Zn] (μM)	123	210	179	205	167	197	172	206
[Fe] (μM)	270	121	195	199	149	182	212	322
% ^{57}Fe	60	72	66	73	57	85	83	58
Hemoglobin Doublet subtracted (%)	37	3	5	10	11	14	11	18
Effective [Fe] in brain (μM)	170	117	185	179	132	157	188	264
Ferritin-like sextet (% of effective Fe)	67	54	51	57	19	42	57	56
Central Doublet (% of effective Fe)	19	27	37	31	57	42	30	33
sextet/CD ratio	3.5	2.0	1.4	1.8	0.33	1.0	1.9	1.7
HS Fe^{II} hemes (% of effective Fe)	~ 0	13	8	6	13	9	7	9
HS Fe^{II} nonheme (% of effective Fe)	10	6	~ 4	6	10	8	6	~ 2
[Fe^{II} heme *a*] (μM)	~ 0	~ 0	4	15	15	18	18	18
[Fe^{II} heme *b*] (μM)	*	~ 0	6	15	12	18	18	18
[Fe^{II} heme *c*] (μM)	~ 0	~ 4	12	23	25	32	32	35
g_{ave} = 4.3 (μM); HS Fe^{III} nonheme	0.1	0.1	0.1	0.1	0.1	0.1	0.1	0.1
g = 1.90 μM); Rieske $[Fe_2S_2]^{1+}$	0	0.9	1.2	1.5	1.5	2.7	2.4	1.7
g = 1.93 (μM); SDH $[Fe_2S_2]^{1+}$	0	1	1.2	1.5	1.5	2.4	2.1	1.5
g = 2.00 (μM); organic radical	0.1	0.1	0.1	0.3	0.3	0.2	0.3	0.7